

Shape transition and oblate-prolate coexistence in $N = Z$ fp -shell nuclei

K. Kaneko¹, M. Hasegawa², and T. Mizusaki³

¹*Department of Physics, Kyushu Sangyo University, Fukuoka 813-8503, Japan*

²*Laboratory of Physics, Fukuoka Dental College, Fukuoka 814-0193, Japan*

³*Institute of Natural Sciences, Senshu University, Kawasaki, Kanagawa, 214-8580, Japan*

(Dated: July 28, 2018)

Nuclear shape transition and oblate-prolate coexistence in $N = Z$ nuclei are investigated within the configuration space ($2p_{3/2}$, $1f_{5/2}$, $2p_{1/2}$, and $1g_{9/2}$). We perform shell model calculations for ^{60}Zn , ^{64}Ge , and ^{68}Se and constrained Hartree-Fock (CHF) calculations for ^{60}Zn , ^{64}Ge , ^{68}Se , and ^{72}Kr , employing an effective pairing plus quadrupole residual interaction with monopole interactions. The shell model calculations reproduce well the experimental energy levels of these nuclei. From the analysis of potential energy surface in the CHF calculations, we found shape transition from prolate to oblate deformation in these $N = Z$ nuclei and oblate-prolate coexistence at ^{68}Se . The ground state of ^{68}Se has oblate shape, while the shape of ^{60}Zn and ^{64}Ge are prolate. It is shown that the isovector matrix elements between $f_{5/2}$ and $p_{1/2}$ orbits cause the oblate deformation for ^{68}Se , and four-particle four-hole ($4p - 4h$) excitations are important for the oblate configuration.

PACS numbers: 21.60.Cs, 21.60.Jz, 21.60.-n, 21.10.-k

The proton-rich nuclei with masses between 56 and 80 are well known to change rapidly their collective properties with proton and neutron numbers. The relevant Nilsson diagram [1] shows a large shell gap for $N, Z = 34$ at prolate and oblate deformations, for $N, Z = 36$ at large oblate deformation, and for $N, Z = 38$ at large prolate deformation. Particular interests are in shape transition and oblate-prolate coexistence of heavier $N = Z$ nuclei. These nuclei lie in the transitional region from the spherical shape (e.g. ^{56}Ni [2]) with coexisting prolate shape [3] to the prolate deformation (e.g. ^{80}Zr [4]). The nucleus ^{64}Ge [5] is known to be an $N = Z$ proton-rich unstable nucleus manifesting a γ -soft structure from the theoretical calculations based on the mean-field approximation. The early studies of ^{69}Se [6] have found indications of oblate shapes. Long standing predictions of a stable oblate deformation were recently confirmed by the observation of an oblate ground state band in ^{68}Se [7]. Determinations of shape were inferred indirectly from the study of rotational bands, while direct quadrupole measurements are difficult for short-lived states. In their analyses, it was suggested that the oblate configuration coexists with a prolate rotational band which is so-called oblate-prolate coexistence. Previous work [8] for ^{72}Kr suggests that the ground state has an oblate shape and there is an oblate \rightarrow prolate shape transition at low spins. In the total Routhian surface (TRS) calculations [9], the oblate minimum can be understood in terms of the large gap for oblate deformation at $N = Z = 36$. Projected shell model [10], a deformed selfconsistent Hartree-Fock (HF)+RPA approach [11], and Skyrme Hartree-Fock-Bogolyubov (HFB) calculations [12] for proton-rich nuclei in the $A = 70$ -80 mass region were performed. Recent investigations for ^{68}Se have been carried out by the projected shell model [13], by the excited VAMPIR method [14], and the self-consistent collective coordinate method [15].

The spherical shell model approaches could be more

appropriate for describing various aspect of nuclear structure. However, the shell model calculations by diagonalization in the $1f_{7/2}$, $2p_{3/2}$, $1f_{5/2}$, $2p_{1/2}$, and $1g_{9/2}$ for nuclei with $N, Z = 30 - 36$ are hopeless at present because of huge dimension of configuration space. So we need to restrict the model space to the $2p_{3/2}$, $1f_{5/2}$, $2p_{1/2}$, and $1g_{9/2}$ orbits (henceforth called fp -shell). The dimension of the configuration space is still huge. For instance, maximum dimension for ^{68}Se is 0.165 billion. Recently, an extended pairing plus quadrupole-quadrupole ($P + QQ$) force has been applied to the fp -shell nuclei, and shown to be useful [16, 17]. This interaction works remarkably well. In this paper, we study the shape transition and oblate-prolate coexistence in the $N = Z$ fp -shell nuclei using a large scale shell model and the constrained Hartree-Fock (CHF) calculations. The shell model calculations with $\sim 10^8$ dimension can be carried out by recently developed shell model code [18]. The observation associated with oblate shape is rare compared with the prolate shape well established experimentally. The reason for the suppression of oblate deformation lies in the higher order effects both in liquid drop terms and residual interactions which make most nuclei favor prolate shapes. Very strong oblate-driving effects seem to be necessary for overcoming this prolate tendency. As a candidate for the oblate-driving force, we present the isovector ($T = 1$) interaction with matrix element between $f_{5/2}$ and $p_{1/2}$ orbits.

We start from the extended $P + QQ$ model [16, 17] with the monopole interactions V_m

$$\begin{aligned} H &= H_0 + H_{P_0} + H_{QQ} + H_{OO} + V_m \\ &= \sum_{\alpha} \varepsilon_{\alpha} c_{\alpha}^{\dagger} c_{\alpha} - \frac{1}{2} g_0 \sum_{\kappa} P_{001\kappa}^{\dagger} P_{001\kappa} \\ &\quad - \frac{1}{2} \chi_2 \sum_M : Q_{2M}^{\dagger} Q_{2M} : - \frac{1}{2} \chi_3 \sum_M : O_{3M}^{\dagger} O_{3M} : \end{aligned}$$

$$-k^0 \sum_{JM,ab} A_{JM00}^\dagger(ab) A_{JM00}(ab) + V_m, \quad (1)$$

$$P_{001\kappa}^\dagger = \sum_a \sqrt{j_a + 1/2} A_{001\kappa}^\dagger(aa), \quad (2)$$

$$A_{JMT\kappa}^\dagger(ab) = [c_a^\dagger c_b^\dagger]_{JMT\kappa} / \sqrt{2}, \quad (3)$$

where ε_a is a single-particle energy, $P_{001\kappa}$ is the $T = 1, J = 0$ pair operator, and Q_{2M} (O_{3M}) is the isoscalar quadrupole (octupole) operator. Each term includes p - n components which play important roles in the $N = Z$ nuclei, due to an isospin-invariance.

The shell model calculations [16, 17] have been performed in a shell model space, which assumes a closed ^{56}Ni core. The neutron single-particle energies of $2p_{3/2}$, $1f_{5/2}$, $2p_{1/2}$, and $1g_{9/2}$ in this fp -shell region can be read from the low-lying states of ^{57}Ni . We used the measured values $\varepsilon_{p_{3/2}} = 0.0$, $\varepsilon_{f_{5/2}} = 0.77$, $\varepsilon_{p_{1/2}} = 1.11$, and $\varepsilon_{g_{9/2}} = 3.70$ in MeV, in our previous paper [16]. However, we have recently obtained a better single particle energy $\varepsilon_{g_{9/2}} = 2.50$ MeV which fits odd-mass Ge isotopes in Refs. [20, 21]. This value is consistent with the report in [22]. Since the above Hamiltonian is assumed to be an isospin-invariant, the proton single-particle energies are taken as the same values as the neutron single-particle energies. We searched force strengths of the extended $P + QQ$ interaction using $\varepsilon_{g_{9/2}} = 2.50$ MeV. The obtained values are as follows:

$$\begin{aligned} g_0 &= 0.270(64/A), & \chi_2 &= 0.250(64/A)^{5/3}/b^4, \\ \chi_3 &= 0.05(64/A)^2/b^6, & k^0 &= 1.44(64/A), \end{aligned} \quad (4)$$

where g_0 , χ_2 , χ_3 , and k^0 are the $J = 0$ pairing, the QQ , the octupole, and J -independent isoscalar force strengths, respectively. Here b is the harmonic-oscillator range parameter. The monopole shifts are

$$\begin{aligned} V_m(p_{3/2}, f_{5/2}; T = 1) &= V_m(p_{3/2}, p_{1/2}; T = 1) = -0.3, \\ V_m(f_{5/2}, p_{1/2}; T = 1) &= -0.4, \\ V_m(g_{9/2}, g_{9/2}; T = 1) &= -0.2, \\ V_m(g_{9/2}, g_{9/2}; T = 0) &= -0.1, \quad \text{in MeV.} \end{aligned} \quad (5)$$

All these force strengths have been phenomenologically adjusted so as to fit many energy levels including high-spin levels for $^{60,62,64,66,68}\text{Zn}$, $^{64,66,68,70}\text{Ge}$ and also $^{65,67}\text{Ge}$ [20, 21]. The force strengths determined in this way describe quite well various properties of these nuclei. In particular, the monopole shifts are important for describing precise positions of the high-spin ($J \geq 8$) states for $^{66,68}\text{Ge}$.

In Fig. 1, energy spectra calculated with the above force strengths are compared with experimental data in the $N = Z$ fp -shell nuclei, ^{60}Zn , ^{64}Ge , and ^{68}Se . In addition to the ground state band, the second positive-parity band beginning from $J^\pi = 2_2^+$ state and negative-parity band beginning from $J^\pi = 3_1^-$ state are shown in Fig. 1. The calculated energy levels are in good agreement with the experimental energy levels, except

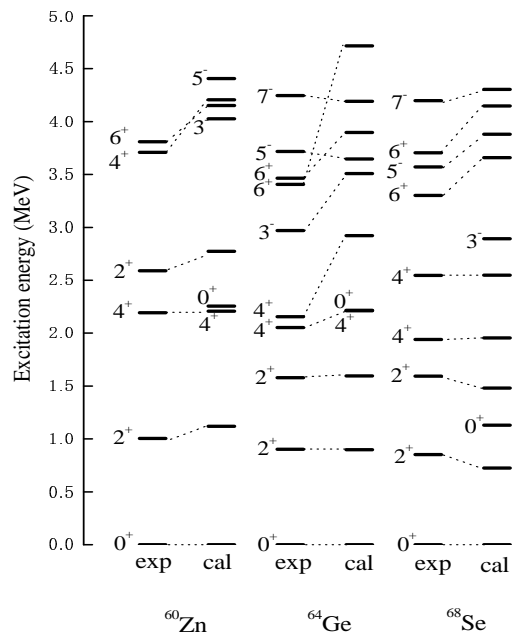


FIG. 1: Experimental and calculated energy levels of ^{60}Zn , ^{64}Ge , and ^{68}Se .

for $J^\pi = 4_2^+$ and $J^\pi = 6_2^+$ levels for ^{64}Ge . In particular, the energy levels of ^{68}Se are well reproduced. The experimental level sequence in the ground-state band shows a quadrupole deformation.

In order to study the quadrupole deformation of these nuclei, we examine the spectroscopic quadrupole moments and $E2$ transitions. We adopted the effective charge $e_p = 1.5e$ for proton and $e_n = 0.5e$ for neutron. Figure 2 shows the calculated spectroscopic quadrupole moments for the first and second excited 2^+ states for ^{60}Zn , ^{64}Ge , and ^{68}Se . The quadrupole deformation was estimated from the spectroscopic quadrupole moments for the first and second excited 2^+ states on the assumption of axially symmetric deformation. For ^{60}Zn and ^{64}Ge , the deformation estimated from the quadrupole moments are prolate with $\beta \sim 0.2$ for the first excited 2^+ state (2_1^+) and oblate with $\beta \sim -0.2$ for the second excited 2^+ state (2_2^+). The nucleus ^{68}Se favors an oblate deformation with $\beta \sim -0.2$ since the value of intrinsic quadrupole moment for the 2_1^+ state becomes negative. On the other hand, the 2_2^+ state has prolate deformation with $\beta \sim 0.2$. The results indicate shape transition in these nuclei. We examined the contributions of interaction matrix elements to the quadrupole moments. We found that the $T = 1$ matrix elements between $f_{5/2}$ and $p_{1/2}$ orbits strongly affect the quadrupole moments. The $T = 1$ monopole interaction is particularly important for the inversion of signs of the quadrupole moments in ^{68}Se . As seen in Fig. (2), the inversion of the quadrupole mo-

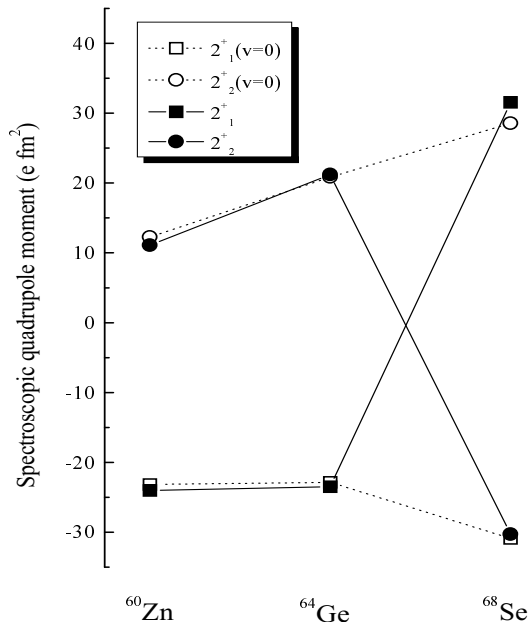


FIG. 2: Spectroscopic quadrupole moments in ^{60}Zn , ^{64}Ge , and ^{68}Se . The solid squares and circles are quadrupole moments of the first and second excited 2^+ states, respectively, obtained by the shell model calculations. The open squares and circles are those obtained by ignoring the $T = 1$ monopole matrix elements.

ments occurs in ^{68}Se , when we remove only the $T = 1$ monopole matrix elements $v = V_m(f_{5/2}, p_{1/2}; T = 1) = -0.4$ MeV from all of the interaction matrix elements. Namely, the shape of ground state in ^{68}Se becomes prolate in this case. Thus, we can say from our calculations that the inverse signs of the quadrupole moments are attributed to the $T = 1$ interaction with matrix element between $f_{5/2}$ and $p_{1/2}$ orbits.

The quadrupole deformation of ^{64}Ge estimated from the calculated $B(E2; 2_1^+ \rightarrow 0_1^+)$ is $\beta \sim 0.2$ [16]. This value is in agreement with the predictions $\beta \sim 0.22$ by Möller and Nix [23], and $\beta \sim 0.22$ by Ennis *et al.* [5]. The calculated value of $B(E2; 2_2^+ \rightarrow 2_1^+)/B(E2; 2_2^+ \rightarrow 0_1^+)$ is very large, which indicates the γ -softness according to the Davydov model [24]. This is in agreement with the γ -softness or triaxiality estimated from the experimental data and the other theoretical models. It was demonstrated [16] that the proton-neutron part $Q_p Q_n$ of the quadrupole-quadrupole interaction is important for the γ -softness or triaxiality. For ^{68}Se , the quadrupole deformation estimated from the calculated $B(E2; 2_1^+ \rightarrow 0_1^+)$ is $\beta \sim 0.21$. The deformations estimated from the quadrupole moment and $B(E2)$ are smaller than $\beta \sim 0.27$ estimated by Fischer *et al.* [7], $\beta \sim 0.30$ obtained by Jenkins *et al.* [25] for ^{69}Se and the value $\beta \sim 0.33$ calcu-

lated by Petrovici *et al.* [14]. This can be attributed to neglect of excitations from the $f_{7/2}$ orbit because of computational limitation.

Let us next examine the nuclear shapes including triaxiality of ^{60}Zn , ^{64}Ge , ^{68}Se , and ^{72}Kr by an alternative approach, the CHF method [3], which is carried out by the following quadratic way:

$$H' = H + \alpha \sum_{\mu} (\langle Q_{2\mu} \rangle - q_{\mu})^2 + \beta (\langle J_x \rangle - j_x)^2, \quad (6)$$

where J_x are the x -component of the angular momentum operator. The q_{μ} 's are the constant parameters $q_0 = \sqrt{\frac{5}{16\pi}} q \cos \gamma$, $q_{\pm 2} = \sqrt{\frac{5}{16\pi}} q \sin \gamma$, and $q_{\pm 1} = 0$, where q is the isoscalar intrinsic quadrupole moment and γ is the triaxial angle. We set $j_x = \sqrt{J(J+1)}$ with J being the total angular momentum of the state. The parameters, α and β , are taken so as to achieve convergence of the iteration of the gradient method. Then, potential energy surface (PES) is defined as the expectation value $\langle H \rangle$ with respect to the CHF state for a given q and γ . Figure 3 shows the contour plots of the PES in the q - γ plane for ^{60}Zn , ^{64}Ge , ^{68}Se , and ^{72}Kr . We can see remarkable shape changes of these nuclei. The PES minimum exhibits prolate deformation for ^{60}Zn and ^{64}Ge , and oblate one for ^{68}Se , and triaxial one for ^{72}Kr . The characteristic features of the PES's are the γ -softness for ^{64}Ge

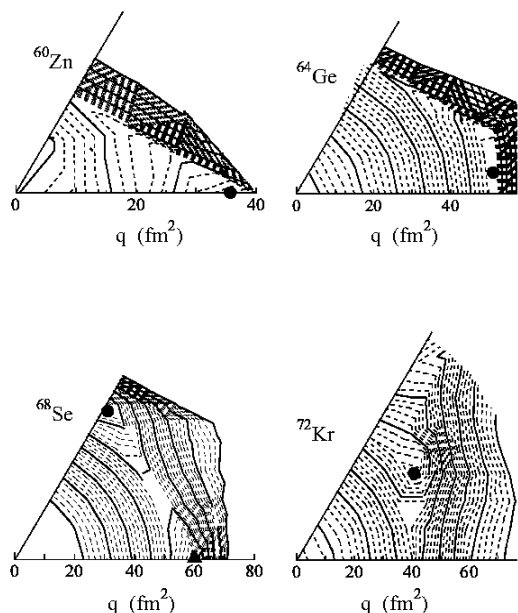


FIG. 3: Contour plots of PES's on q - γ plane in the CHF calculations for ^{60}Zn , ^{64}Ge , ^{68}Se , and ^{72}Kr . The solid circles denote the PES minima, and the solid triangle the second minimum.

and oblate-prolate coexistence for ^{68}Se , which are consistent with the previous discussions [5, 7]. Moreover, we calculated an angular-momentum projected PES which is obtained by calculating the expectation value $\langle H \rangle$ with respect to the angular-momentum projected CHF wave function for a given q and γ . The angular-momentum projection method improves considerably the ground-state energies. The angular-momentum projected PES's show a similar potential energy surface to the CHF.

The PES's as a function of q along the axially symmetric line are shown for ^{60}Zn , ^{64}Ge , ^{68}Se , and ^{72}Kr in Fig. 4. This figure shows the aspect of shape coexistence and shape changes in these nuclei, from different angle. Figure 4 also shows that if the $T = 1$ monopole interactions are removed, the minima of the PES's in ^{68}Se and ^{72}Kr shift to the prolate side, while it remains unchanged in ^{60}Zn , ^{64}Ge . Thus the $T = 1$ monopole interactions with the matrix element $V_m(f_{5/2}, p_{1/2}; T = 1)$ are confirmed to be the oblate-driving force for ^{68}Se and ^{72}Kr . The shape of the ground state becomes oblate for ^{68}Se where the Fermi energy for neutron lies between the $f_{5/2}$ and $p_{1/2}$ orbits. The CHF calculation shows that the shape of ^{72}Kr is triaxial, while it is oblate in the HFB result [12] and the TRS results [8]. Note that the PES of ^{72}Kr is flat toward oblate shape and shows gamma softness,

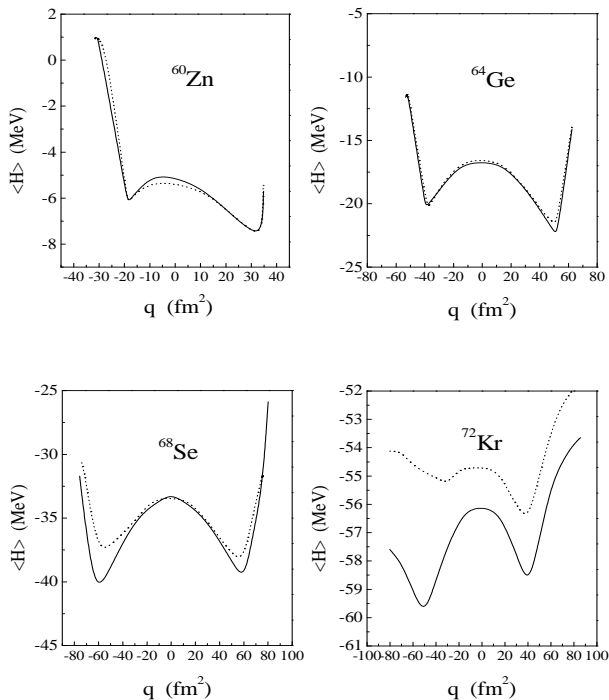


FIG. 4: PES's as a function of q along the axially symmetric line. The solid curves are the PES's in the full shell model matrix elements and the dotted curves are those obtained by ignoring the $T = 1$ monopole matrix element between $f_{5/2}$ and $p_{3/2}$.

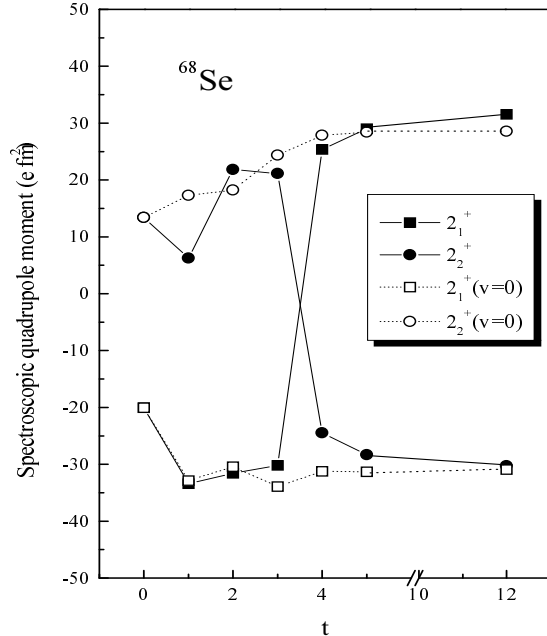


FIG. 5: Spectroscopic quadrupole moment as a function of t . The solid squares and circles are for the first and second excited 2^+ states, respectively. The open squares and circles are those obtained by ignoring the $T = 1$ monopole matrix elements.

as seen in Fig. 3.

We next analyze how excitations from the orbits $(p_{3/2}, f_{5/2})$ to $(p_{1/2}, g_{9/2})$ contribute to the oblate deformation. We calculate the quadrupole moments by enlarging configuration space in the truncation scheme $\bigoplus_{s \leq t} (p_{3/2} f_{5/2})^{A-56-s} (p_{1/2} g_{9/2})^s$, where t is the maximum number of particles allowed to be excited. Figure 5 shows the spectroscopic quadrupole moments as a function of t for ^{68}Se . The spectroscopic quadrupole moment is negative for 2^+_1 for 2^+_2 when $t \leq 3$, but suddenly their signs change at $t=4$. This means that the four-particle four-hole ($4p - 4h$) excitations from $(p_{3/2} f_{5/2})$ to $(p_{1/2} g_{9/2})$ are very important for the oblate configurations. Such a change does not occur when the $T = 1$ monopole interactions are removed, as shown by the dotted lines in Fig. 4. Table I shows the occupation numbers of the $2p_{3/2}$, $1f_{5/2}$, $2p_{1/2}$, and $1g_{9/2}$ orbits for the first and second excited 2^+ states of ^{60}Zn and ^{68}Se in the cases of the $T = 1$ monopole force strengths $v = -0.4$ MeV and 0.0 MeV. When we add the $T = 1$ monopole force, the occupation number of $p_{1/2}$ for the first excited 2^+ state for ^{68}Se increases remarkably. Thus the $T = 1$ monopole force contributes to $4p - 4h$ excitations from $(p_{3/2} f_{5/2})$ to $p_{1/2}$, which is especially important for the oblate configuration.

Our conclusion is different from that of the VAMPIR

TABLE I: Occupation numbers in the first and second excited 2^+ states for ^{60}Zn and ^{68}Se .

^{60}Zn	2_1^+				2_2^+			
	$p_{3/2}$	$f_{5/2}$	$p_{1/2}$	$g_{9/2}$	$p_{3/2}$	$f_{5/2}$	$p_{1/2}$	$g_{9/2}$
$v=-0.4$	0.98	0.51	0.49	0.02	1.08	0.59	0.24	0.09
$v=0.0$	1.06	0.46	0.46	0.02	1.11	0.56	0.24	0.09
^{68}Se	2_1^+				2_2^+			
	$p_{3/2}$	$f_{5/2}$	$p_{1/2}$	$g_{9/2}$	$p_{3/2}$	$f_{5/2}$	$p_{1/2}$	$g_{9/2}$
$v=-0.4$	2.31	2.38	1.20	0.11	2.37	2.81	0.69	0.13
$v=0.0$	2.65	2.78	0.42	0.15	2.70	2.33	0.80	0.15

calculations [14], where the oblate-driving force for ^{68}Se is in monopole shifts for $T = 0$ matrix elements between the $g_{9/2}$ and $f_{5/2}(f_{7/2})$ orbits. We examined this question by changing monopole shifts and single-particle energy $\varepsilon_{g_{9/2}}$. The investigations of the Q moments show that the monopole shift $V_m(f_{5/2}, g_{9/2}; T = 0)$ hardly contributes to the oblate deformation under the single-particle energies adopted in this paper. If we lower $\varepsilon_{g_{9/2}}$ below $\varepsilon_{p_{1/2}}$ as done in Ref. [14], many nucleons occupy the $g_{9/2}$ orbit and $V_m(f_{5/2}, g_{9/2}; T = 0)$ contributes to the oblate deformation. The nucleon occupation numbers of the $p_{1/2}$ and $g_{9/2}$ orbits and phases of respective components of wavefunctions affects the sign of the Q moments. It seems that the VAMPIR conclusion depends on the inversion of $\varepsilon_{p_{1/2}}$ and $\varepsilon_{g_{9/2}}$.

Finally, we discuss shortly standard $P + QQ$ force model calculations neglecting the octupole force and the monopole shifts. We set the force parameters such as so as to reproduce the energy levels of ground-state band for ^{68}Se . Note that the quadrupole force strength is larger than that in Eq. (4). Then, we obtain the positive spec-

troscopic quadrupole moment for the 2_1^+ state and negative one for the 2_2^+ state. Similarly in the CHF calculations, the first PES minimum is in the oblate side and the second minimum is in the prolate side. However, the standard $P + QQ$ force model cannot consistently reproduce the energy levels of the side band for ^{68}Se and the ground-state bands for ^{60}Zn and ^{64}Ge .

In conclusion, we investigated nuclear shape transition and oblate-prolate coexistence in $N = Z$ fp g-shell nuclei. We analyzed the quadrupole moments in the shell model and the CHF calculations. The analysis shows that the $T = 1$ monopole interactions with the matrix element between $f_{5/2}$ and $p_{1/2}$ orbits play an important role in producing the oblate shape for ^{68}Se and ^{72}Kr , while they do not play the same role for ^{60}Zn and ^{64}Ge . Note that this conclusion is different from that of the VAMPIR calculations by Petrovici *et al.*, where the origin of oblate-driving force is $T = 0$ monopole matrix elements between $g_{9/2}$ and $f_{5/2}(f_{7/2})$ orbits. However, in our calculation we could not find any large influence from these $T = 0$ monopole matrix elements on the oblate deformation. The shape transition and oblate-prolate coexistence in the CHF calculations are consistent with those of the Skyrme HFB calculations [12]. The present calculations show that the oblate deformation originates in the $4p-4h$ excitations from $(p_{3/2}f_{5/2})$ to $(p_{1/2}g_{9/2})$. We can expect that the $T = 1$ monopole interactions between $f_{5/2}$ and $p_{1/2}$ orbits are also important for the oblate or triaxial deformation in $N \neq Z$ nuclei where the Fermi surface for neutron lies between $f_{5/2}$ and $p_{1/2}$ in fp g shell. Further investigations are in progress.

-
- [1] W. Nazarewicz, J. Dudek, R. Bengtsson, T. Bengtsson, and I. Ragnarsson, Nucl. Phys. **A435**, 397(1985).
[2] D. Rudolph *et al.*, Phys. Rev. Lett. **82**, 3763 (1999).
[3] T. Mizusaki, T. Otsuka, Y. Utsuno, M. Honma, and T. Sebe, Phys. Rev. C **59**, R1846(1999).
[4] C. J. Lister *et al.*, Phys. Rev. Lett. **59**, 1270 (1987).
[5] P. J. Ennis, C. J. Lister, W. Gelletly, H. G. Price, B. J. Varley, P. A. Butler, T. Hoare, S. Cwoik, and W. Nazarewicz, Nucl. Phys. **A535**, 392 (1991).
[6] M. Wiosna, J. Busch, J. Eberth, M. Liebchen, T. Mylaeus, N. Schmal, R. Sefzig, S. Skoda, and W. Teichert, Phys. Lett. B **200**, 255(1988).
[7] S. M. Fischer, D. P. Balamuth, P. A. Hausladen, C. J. Lister, M. P. Carpenter, D. Seweryniak, and J. Schwartz, Phys. Rev. Lett. **84**, 4064(2000).
[8] G. de Angelis *et al.*, Phys. Lett. B **415**, 217(1997); Nucl. Phys. **A630**, 426c(1998).
[9] E.A. Stefanova *et al.*, Phys. Rev. C **67**, 054319 (2003).
[10] R. Palit, J. A. Sheikh, Y. Sun, and H. C. Jain, Nucl. Phys. **A686**, 141(2001).
[11] P. Sarriguren, E. Moya de Guerra, and A. Escuderos, Nucl. Phys. **A658**, 13(1999).
[12] M. Yamagami, K. Matsuyanagi, and M. Matsuo, Nucl. Phys. **A693**, 579(2001).
[13] Y. Sun, J. Y. Zhang, M. Guidry, J. Meng, and S. Im, Phys. Rev. C **62**, 021601(R)(2000).
[14] A. Petrovici, K. W. Schmid, and A. Faessler, Nucl. Phys. **A710**, 246(2002).
[15] M. Kobayashi, T. Nakatsukasa, M. Matsuo, and K. Matsuyanagi, Prog. Theor. Phys. **110**, 65(2003); nucl-th/0405039.
[16] K. Kaneko, M. Hasegawa and T. Mizusaki, Phys. Rev. C **66**, 051306(R)(2002).
[17] M. Hasegawa, K. Kaneko, T. Mizusaki, and S. Tazaki, Phys. Rev. C **69**, 034324(2004).
[18] T. Mizusaki, RIKEN Accel. Prog. Rep. **33**, 14 (2000).
[19] D. Rudolph, *et al.*, Eur. Phys. J. A **6** (1999), 377.
[20] M. Hasegawa, K. Kaneko, and T. Mizusaki, to be published in Phys. Rev. C, nucl-th/0408062 (2004).
[21] M. Hasegawa, K. Kaneko, and T. Mizusaki, nucl-th/0408063 (2004).
[22] A. Juodagalvis and S. Aberg, Nucl. Phys. **A683**, 206(2001).
[23] P. Möller and J. R. Nix, At. Data Nucl. Data Tables **26**, 165 (1981).
[24] A. S. Davydov and G. F. Filippov, Nucl. Phys. **8**,237 (1958).
[25] D. G. Jenkins, D. P. Balamuth, M. P. Carpenter, C. J.

Lister, S. M. Fischer, R. M. Clark, A. O. Macchiavelli, P. Fallon, C. E. Svensson, N. S. Kelsall, and R. Wadsworth,

Phys. Rev. C **64**, 064311(2001).